

Review

Carbon Dots for Sensing and Killing Microorganisms

Fengming Lin, Yan-Wen Bao and Fu-Gen Wu * 

State Key Laboratory of Bioelectronics, School of Biological Science and Medical Engineering,
Southeast University, Nanjing 210096, China; linfengming@seu.edu.cn (F.L.); byw@seu.edu.cn (Y.-W.B.)

* Correspondence: wufg@seu.edu.cn; Tel.: +86-025-8379-1810

Received: 12 April 2019; Accepted: 29 May 2019; Published: 14 June 2019



Abstract: Carbon dots (or carbon quantum dots) are small (less than 10 nm) and luminescent carbon nanoparticles with some form of surface passivation. As an emerging class of nanomaterials, carbon dots have found wide applications in medicine, bioimaging, sensing, electronic devices, and catalysis. In this review, we focus on the recent advancements of carbon dots for sensing and killing microorganisms, including bacteria, fungi, and viruses. Synthesis, functionalization, and a toxicity profile of these carbon dots are presented. We also discuss the underlying mechanisms of carbon dot-based sensing and killing of microorganisms.

Keywords: C-dots; CDs; antibacterial; antimicrobial; biofilm

1. Introduction

The spread of infectious diseases is a growing and persistent threat to human health, aggravated by microbial resistance to antibiotics [1]. The development of novel microbial probes and antimicrobial materials is highly desirable in this era of ever-increasing antibiotic resistance [2,3]. Recently, antimicrobial nanomaterials have offered new opportunities to treat infectious diseases. Among them, carbon dots (or carbon quantum dots), which are carbon nanoparticles with sizes smaller than 10 nm, are considered as appealing agents for microbial imaging, detection, and inactivation due to their excellent optical properties, modifiable surfaces, and good biocompatibility [4].

Carbon dots (CDs) were accidentally found during the purification of single-walled carbon nanotubes [5]. Since then, CDs have become an attractive class of photoluminescent nanoagents with wide applications in nanomedicine [6–11], bioimaging [7,10–15] catalysis [16], optoelectronics [17], and sensing [15]. Various starting materials have been used to synthesize CDs via different routes over the past few years. The most popular approaches are microwave-mediated synthesis, hydrothermal synthesis, laser ablation of graphite, electrooxidation of graphite, oxidation of candle soot, and thermal cracking of organic compounds [18,19]. Among them, hydrothermal synthesis is the most commonly used approach for CD fabrication because it is simple and efficient. Furthermore, the surface and carbogenic core of CDs can be easily modified by versatile engineering methods to endow the CDs with desired physicochemical and optical properties. Despite the growing attention to the biological applications of CDs, a review focusing on their applications in imaging and killing microorganisms is still lacking. In this review, we summarize the recent progress on the applications of CDs as microbial probes and antimicrobial agents. As far as we know, the current researches on using CDs for imaging and killing microorganisms are mainly on bacteria, and only several studies are about fungi [20–25] and viruses [26–30]. Therefore, this review mainly focuses on the interactions between CDs and bacteria.

2. CDs for Sensing Microorganisms

Imaging microorganisms with fluorescence techniques is a popular way to study their structure and state, which is important for the quantification, viability testing, and Gram type determination of

microorganisms. CDs display bright fluorescence emission in the visible and near-infrared spectral range. Some CDs display distinctive excitation-dependent fluorescence emission with wide excitation spectra [31], which can be used for multicolor fluorescence imaging. In addition, CDs usually possess fascinating attributes, such as high photoluminescence, weak photobleaching, low toxicity, and good stability, which make them promising imaging probes for microbial sensing [2]. Here, we present microbial detection using fluorescent CDs via different mechanisms, and the related applications, including microbial detection, viability testing, Gram type determination, and biofilm imaging (Figure 1).

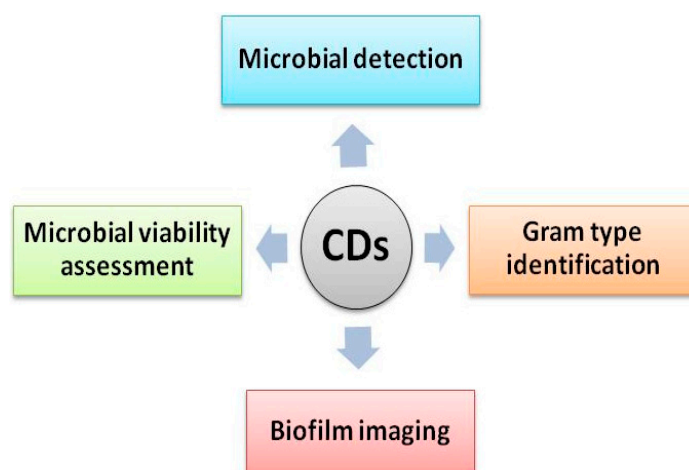


Figure 1. Carbon dots (CDs) for sensing microorganisms.

2.1. Microbial Detection

Bare CDs themselves can enter and light up microbial cells due to their small size, positive charge, amphiphilic affinity, and surface functional groups from starting materials. In addition, functionalized CDs for microbial labeling can be obtained by modifying the surface of CDs with antibiotics [32,33] or integrating with other nanomaterials, like hydrogels [34] or magnetic nanoparticles [35].

2.1.1. CDs Derived from Natural Sources for Microbial Imaging

It has been reported that fluorescent CDs can be synthesized from different natural sources, which is cost-effective for bulk preparation, and the obtained CDs have great biocompatibility. For example, using the one-step hydrothermal method, natural sources like *Punica granatum* fruits [20], *Saccharum officinarum* juice [21], *Carica papaya* juice [22], egg whites [36], and rice straw [37] were utilized as precursors to prepare CDs for bacterial labeling. These CDs have been successfully used to image bacterial cells, such as *Escherichia coli* (*E. coli*) [21,36], *Staphylococcus aureus* (*S. aureus*) [36], *Pseudomonas aeruginosa* (*P. aeruginosa*) [20], and *Bacillus subtilis* (*B. subtilis*) [22], and fungal cells such as *Saccharomyces cerevisiae* (*S. cerevisiae*) [21], *Fusarium sporotrichioides* (*F. sporotrichioides*) [20], and *Aspergillus aculeatus* (*A. aculeatus*) [22]. The incubation time for the microbial labeling of these CDs is short—in the range of 2–10 min [20,21,36]. Sometimes, microbial cells need to be fixed using 70% ethanol before incubation with CDs [20–22]. Nevertheless, the underlying mechanisms of the microbial imaging using these fluorescent CDs remain to be explored.

In addition to these CDs derived from natural materials, other non-natural product-derived CDs prepared from pollutant soot of diesel engine exhaust with chemical oxidation [38], bulk fluorine-doped carbon nitride powder in ethylene glycol via sonication treatment [39], and citric acid and amino compounds containing hydroxyl groups such as tris(hydroxymethyl)aminomethane and ethanolamine by a one-step microwave process [40] have been successfully used to image *E. coli* cells.

2.1.2. Amphiphilic CDs for Microbial Monitoring

Amphiphilic CDs contain both hydrophobic and hydrophilic parts and have high affinity for microbial surfaces, enabling microbial monitoring via both fluorescence spectroscopy and microscopy. In 2015, Nandi et al. used amphiphilic CDs for bacterial detection [41]. The 6-*O*-Acylated fatty acid ester of D -glucose was prepared by reacting D -glucose with *O,O'*-di-lauroyl-tartaric acid anhydride and carbonized to yield amphiphilic CDs. Interestingly, the fluorescence of CDs was sensitive to bacterial species with its intensity and spectral position changed for different microorganisms, which is consistent with a previous finding that the fluorescence of CDs was sensitive to their environment [42,43]. Thus, they can be utilized to distinguish different bacteria in mixed bacterial populations. The bacterial detection threshold of these CDs is 10^3 – 10^5 cells/mL. However, the biocompatibility of these amphiphilic CDs has not been investigated, and whether these CDs can affect and/or kill the labeled microorganisms has not been studied. When these amphiphilic CDs were mixed with their precursor 6-*O*-acylated fatty acid ester of D -glucose in water, a new hybrid CD–hydrogel material was formed after gelation [34]. The amphiphilic CDs were well dispersed within the hydrogel matrix due to their affinity for the amphiphilic and hydrophobic domains on the internal porous surface (Figure 2). The hydrogel-dispersed CDs displayed increased fluorescence, since they were not aggregated [44,45]. However, in bacterial suspensions, the ester bonds of the hydrogel scaffold were cleaved by bacterially secreted esterases and lipases, and the hydrogel was fluidized, resulting in the aggregation and concomitant fluorescence quenching of the embedded CDs. In this way, the CD–hydrogel was applied for bacterial detection. This assay can be employed to distinguish bacterial species with varied abilities of esterase/lipase secretion.

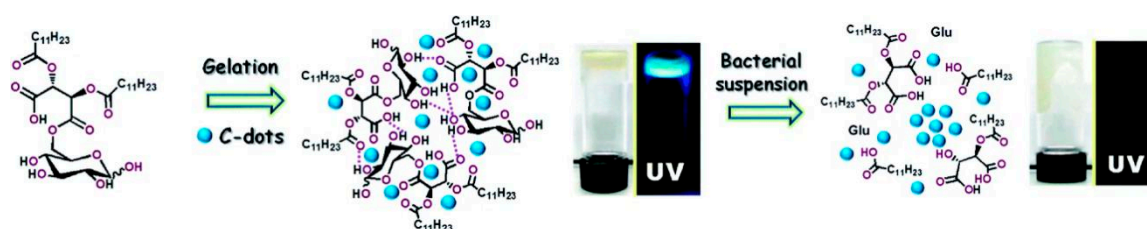


Figure 2. Hybrid CD–hydrogel composite for bacterial detection. Reproduced with permission from [34]. Copyright Royal Society of Chemistry, 2017.

2.1.3. Functionalized CDs for Microbial Labeling

Pristine CDs usually contain carboxyl, hydroxyl, and amino groups on their surfaces, enabling facile surface modification to prepare functionalized CDs [46]. Functionalized CDs integrated with magnetic nanoparticles [35], antibiotics such as colistin [32] and amikacin [33], and mannose [47], have been synthesized for microbial labeling. CD-coated magnetic nanoparticles (Mag-CDs) were prepared by decorating magnetic nanoparticles with CDs made from chitosan, and the resultant Mag-CDs possessed both fluorescence and magnetic properties [35]. The precursor chitosan provides Mag-CDs with amine groups that are poly-cationic and can remarkably interact with the negatively charged bacteria by electrostatic interaction, hydrophobic interaction, and hydrogen bonding. Therefore, these amine-functionalized Mag-CDs successfully detected and identified bacterial strains *S. aureus* and *E. coli* in both phosphate-buffered saline and urine with either fluorescence spectroscopy or matrix-assisted laser desorption/ionization mass spectrometry. The limit of detection (LOD) for *S. aureus* and *E. coli* was 3×10^2 and 3.5×10^2 CFU/mL, respectively. It is worth noting that the incubation time was very short; only 2 min was used for the labeling and enrichment of the bacteria.

Colistin, a famous cyclic polypeptide antibiotic against Gram-negative bacteria, was adopted as a binding ligand for *E. coli* to selectively detect this bacterial strain [32]. Colistin-conjugated CDs (CDs@colistin) were synthesized by carbonization of solid ammonium citrate in the presence of colistin. The LOD of CDs@colistin for *E. coli* varied with different samples but was in the range of 460–640 CFU/mL. CDs@colistin displayed rapid, selective, and sensitive detection in real samples, such as tap water, apple juice, and human urine. CDs@colistin could specifically detect Gram-negative

bacteria because its colistin units can interact with the lipopolysaccharide molecules in the outer membrane of the bacteria. Moreover, mannose, which selectively binds to the FimH lectin unit in the flagella of the wild-type *E. coli* K12 strain [47], and amikacin, which is a synthetic amino glycoside antibiotic against Gram-negative bacteria [33], were applied to modify CDs for the selective detection of *E. coli*.

2.2. Gram Type Identification Using CDs

Gram staining is the traditional way to identify unknown bacteria, classifying bacterial species into two categories: Gram-positive and Gram-negative ones [48]. Gram type identification is important, since it can dictate which antibiotics are used to treat bacterial infections. Nevertheless, this strategy has several drawbacks, including false positive results and laborious processes. Functionalized fluorescent CDs can be employed to identify Gram types in a more convenient and rapid way. For example, CDs functionalized with vancomycin [49] or lauryl betaine [50] were used for the selective detection of Gram-positive bacteria. Zhong et al. prepared CDs from citric acid and urea using microwave-assisted hydrothermal treatment [49]. The as-synthesized CDs were modified with vancomycin through amide coupling, generating vancomycin-conjugated CDs (CDs@Van) (Figure 3A). CDs@Van successfully detected *S. aureus* with a linear range of 3.18×10^5 – 1.59×10^8 CFU/mL and an LOD of 9.40×10^4 CFU/mL. CDs@Van showed high selectivity for imaging Gram-positive bacteria. Vancomycin is a broad-spectrum glycopeptide antibiotic that can bind to the terminal peptide D-Ala-D-Ala on the cell wall of Gram-positive bacteria. Therefore, CDs@Van aggregated on the surface of Gram-positive bacteria, causing fluorescence quenching (Figure 3A). Yang et al. fabricated quaternized CDs by coupling lauryl betaine with amine-terminated CDs via a carboxyl–amine reaction (Figure 3B) [50]. The amine-terminated CDs were produced by solvothermal treatment of 3-[2-(2-aminoethylamino)ethylamino]propyl-trimethoxysilane (AEEA) and glycerol. The quaternized CDs selectively labeled Gram-positive bacteria instead of Gram-negative ones, simply and rapidly distinguishing Gram-positive and Gram-negative bacteria using fluorescence microscopy or flow cytometry. In a very recent report, Yang et al. developed a one-pot solvothermal method to prepare a new type of quaternized CDs using dimethyloctadecyl[3-(trimethoxysilyl)propyl]ammonium chloride (Si-QAC) and glycerol (Figure 3C) [51]. The CDs could selectively interact with Gram-positive bacteria and the bacterial adsorption could significantly enhance their fluorescence emission, thus efficiently distinguishing Gram-positive and Gram-negative bacteria via fluorescence imaging.

To selectively image Gram-negative bacteria, Chandra et al. prepared amikacin-modified fluorescent CDs (CDs@amikacin) by hydrothermal carbonization of di-ammonium hydrogen citrate and amikacin [33]. Amikacin is a widely used amino glycoside antibiotic against Gram-negative bacteria. CDs@amikacin could image *E. coli* well but not *S. aureus*. The fluorescence intensity of CDs@amikacin showed a linear relationship with *E. coli* concentration in the range of 7.625×10^2 – 3.904×10^5 with an LOD of 552 CPU/mL. In addition, CDs@amikacin were successfully applied for *E. coli* detection in fruit samples, like orange, apple, and pineapple. Compared with the conventional Gram staining method that includes three-step labeling with three dyes and is labor-intensive [48], the selective Gram type identification by CDs is faster and simpler for distinguishing bacteria.

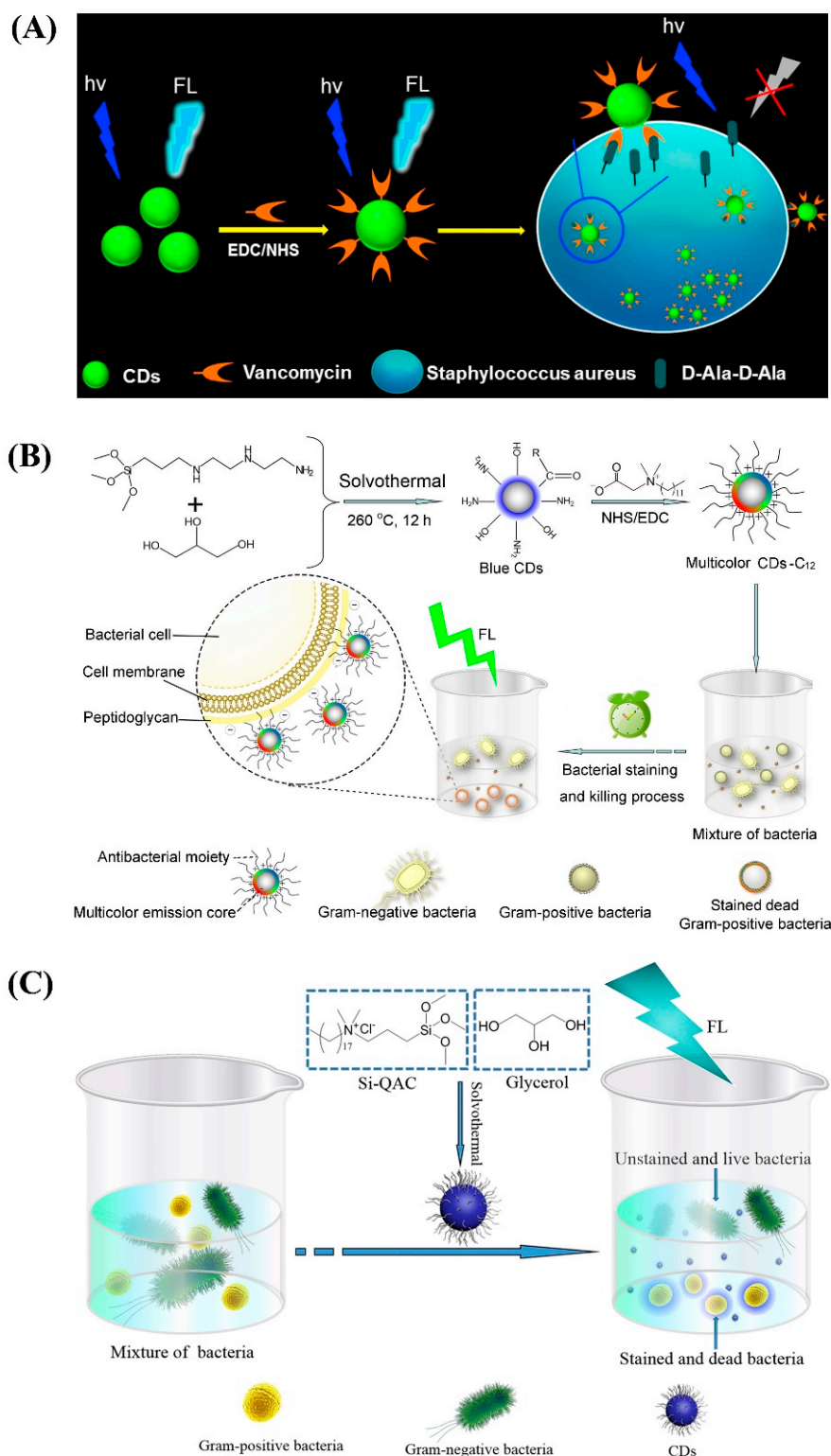


Figure 3. (A) Schematic demonstration of vancomycin-conjugated CDs (CDs@Van)-based strategy for selectively imaging Gram-positive bacteria, as exemplified by *S. aureus*. Reproduced with permission from [49]. Copyright Elsevier, 2015. (B) Schematic showing the synthesis of multicolor amine-terminated CDs and their application in selective imaging and killing of Gram-positive bacteria. Reproduced with permission from [50]. Copyright American Chemical Society, 2016. (C) Schematic demonstrating the fabrication of quaternized CDs and their application in selective Gram-positive bacterial imaging and killing. Reproduced with permission from [51]. Copyright Elsevier, 2019.

2.3. Microbial Viability Assessment Using CDs

In industrial and biomedical fields, microbial viability tests are frequently carried out for microbial monitoring, antibiotic development, and pathogen detection. Usually, plate counting, which has relatively low sensitivity and accuracy, is performed to assay microbial viability [52]. Meanwhile, the whole process is labor-intensive and time-consuming. To solve these issues, efforts have been devoted to developing novel ways to discriminate between live and dead microorganisms. Newly-developed strategies, such as nucleic acid sequence-based amplification [53], Fourier-transform infrared spectroscopy [54], atomic force microscopy [55], and surface-enhanced Raman scattering [56], can achieve higher accuracy than plate counting. Nevertheless, these methods require the pretreatment of microorganisms, which is costly and time-consuming. In contrast, fluorescent dye labeling combined with flow cytometry or fluorescence microscopy is simple, fast, visible, and sensitive and is therefore considered as a promising alternative to plate counting. The commercial dyes used in this method, like propidium iodide and propidium monoazide, have the disadvantages of cumbersome processes, photobleaching, instability, toxicity, or high cost. Thus, it is highly desirable to develop new probes for microbial viability testing.

CDs are emerging as promising probes for microbial viability assays. Several studies have successfully employed fluorescent CDs as probes to evaluate microbial viability [23,57–59]. Hua et al. synthesized fluorescent CDs from bacteria via hydrothermal treatment (Figure 4A), which is simple, eco-friendly, and inexpensive [23]. The small size (3–5 nm) and highly negatively charged surfaces (zeta potential: -42 mV) of the CDs enable them to stain dead bacteria and fungi but not live ones. These CDs have advantages including great photostability, multicolor imaging ability, and low cytotoxicity, representing a promising probe for fluorescence-based microbial viability evaluation. Nitrogen, phosphorus, and sulfur co-doped CDs (NPSCDs) were prepared through one-step hydrothermal reaction of a yeast extract with a high quantum yield of 32% [57]. NPSCDs have similar properties and advantages to the CDs derived from bacteria. Interestingly, the fluorescence of the NPSCDs decreased linearly as temperature increased from 30 °C to 90 °C (Figure 4B) and recovered with decreasing temperature. Moreover, NPSCDs monitored a remarkable reduction of bacterial viability upon heating at 60 °C for 15 min (Figure 4C,D), demonstrating that the CDs could selectively label dead bacteria in real time. Four types of nitrogen and phosphorus co-doped CDs (NPCDs) with tunable surface charges were fabricated by hydrothermal treatment of yeast extract in the presence of ethylenediamine, citric acid, melamine, and ammonia water, respectively [58]. NPCDs could stain dead bacteria but not live ones. More accurate mortality was obtained using NPCDs with more negatively charged surfaces. In another report, bacterial extracellular polymeric substances (EPSs) were used to prepare fluorescent N-doped CDs (CDs-EPS605) via a facile one-step hydrothermal method [59]. CDs-EPS605 were found to selectively stain dead microorganisms but not live ones, enabling live/dead microorganisms to be distinguished.

Collectively, all of the above examples used natural sources like bacteria [23], yeast extracts [57,58], and EPSs [59] to prepare highly negatively charged CDs through the one-step hydrothermal method. The synthesis of these CDs is simple and cost-effective, and the microbial viability evaluation via the CDs is sensitive (even at a single cell level) and accurate.

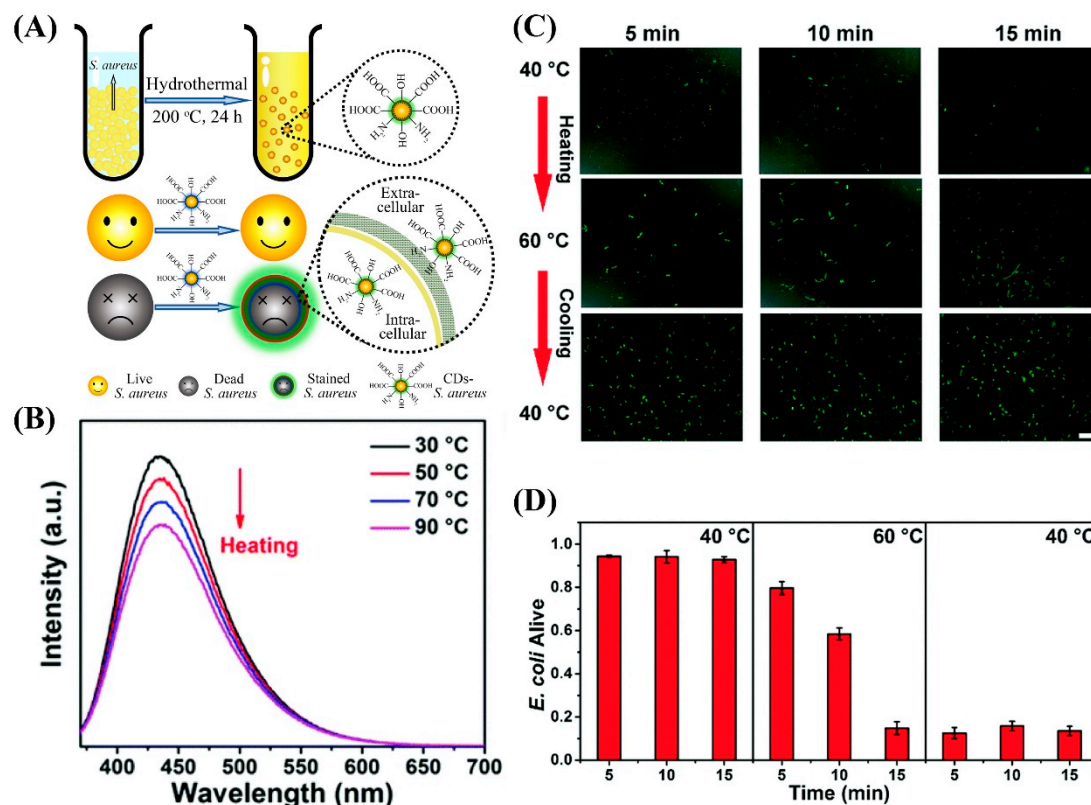


Figure 4. (A) Schematic of preparation and selective dead bacterial staining of CDs-*S. aureus*. Reproduced with permission from [23]. Copyright Royal Society of Chemistry, 2017. (B) Fluorescence spectra of nitrogen, phosphorus, and sulfur co-doped CDs (NPSCDs) under heating. (C) Confocal images of *E. coli* cells under various conditions and (D) corresponding rates of live *E. coli* in (C) with three replicates. The figures in (B–D) are reproduced with permission from [57]. Copyright Royal Society of Chemistry, 2017.

2.4. CDs for Biofilm Imaging

Biofilms are multicellular communities assembled by microorganisms on surfaces in natural, industrial, and clinical environments [60]. In biofilms, microorganisms are encased in a sticky and strong EPS matrix that mainly comprises polysaccharides, proteins, lipids, and DNA [60]. Biofilms are more recalcitrant to environmental stresses, antibiotics, and immune defenses than planktonic cells [61]. Biofilms can cause chronic human infections, implant failure, antibiotic resistance, and even human death [62]. In addition, biofilms may damage industrial facilities by corroding pipes, blocking filtration membranes, and fouling marine surfaces [63]. However, it is still very challenging to reveal the mechanisms behind biofilm formation and dispersal, let alone to treat the biofilms. To solve these challenges, there is an urgent need to develop new analytic techniques for biofilms.

EPSs form the physical scaffolds of microorganism biofilms and play a central role in biofilm development and virulence. Current techniques for EPS visualization, such as Raman microscopy, scanning electron microscopy, atomic force microscopy, and magnetic resonance imaging, cannot realize in situ measurements but require sample pretreatments and only give partial structural details [64,65]. On the other hand, the existing probes for fluorescence microscopy analysis of EPSs are toxic to bacterial cells, including dyes covalently linked to carbohydrate recognition elements [66] and surface-functionalized semiconductor quantum dots [67,68]. This not only damages mature biofilms but also prevents in situ visualization of EPSs. In contrast, amphiphilic CDs that are less toxic can image the EPSs in situ without the need for sample pretreatments. Amphiphilic fluorescent CDs made from 6-*O*-acylated fatty acid ester of D-glucose via hydrothermal carbonization can bind to and light up the EPS of *P. aeruginosa* biofilm, allowing visualization of the EPS structure via fluorescence microscopy [69]. It has been revealed that *P. aeruginosa* EPS matrix features a notable dendritic morphology. The CDs

successfully monitored in real time the growth kinetics of the EPSs and how they were affected by external factors, such as temperature and biofilm inhibitors.

Except EPSs, microorganisms within biofilms can also be labeled by fluorescent CDs developed by our group [70]. We previously synthesized CDs from *Lactobacillus plantarum* (*L. plantarum*) by one-step hydrothermal carbonization. The obtained CDs were termed CDs-605, which can successfully visualize the microorganisms of biofilms, including Gram-negative bacteria (*E. coli* and *Shewanella oneidensis* (*S. oneidensis*)), Gram-positive bacteria (*P. aeruginosa* and *S. aureus*), and *Trichoderma reesei* (*T. reesei*) (Figure 5). CDs-605 did not interfere with the biofilms and exhibited better photostability than commercial dyes.

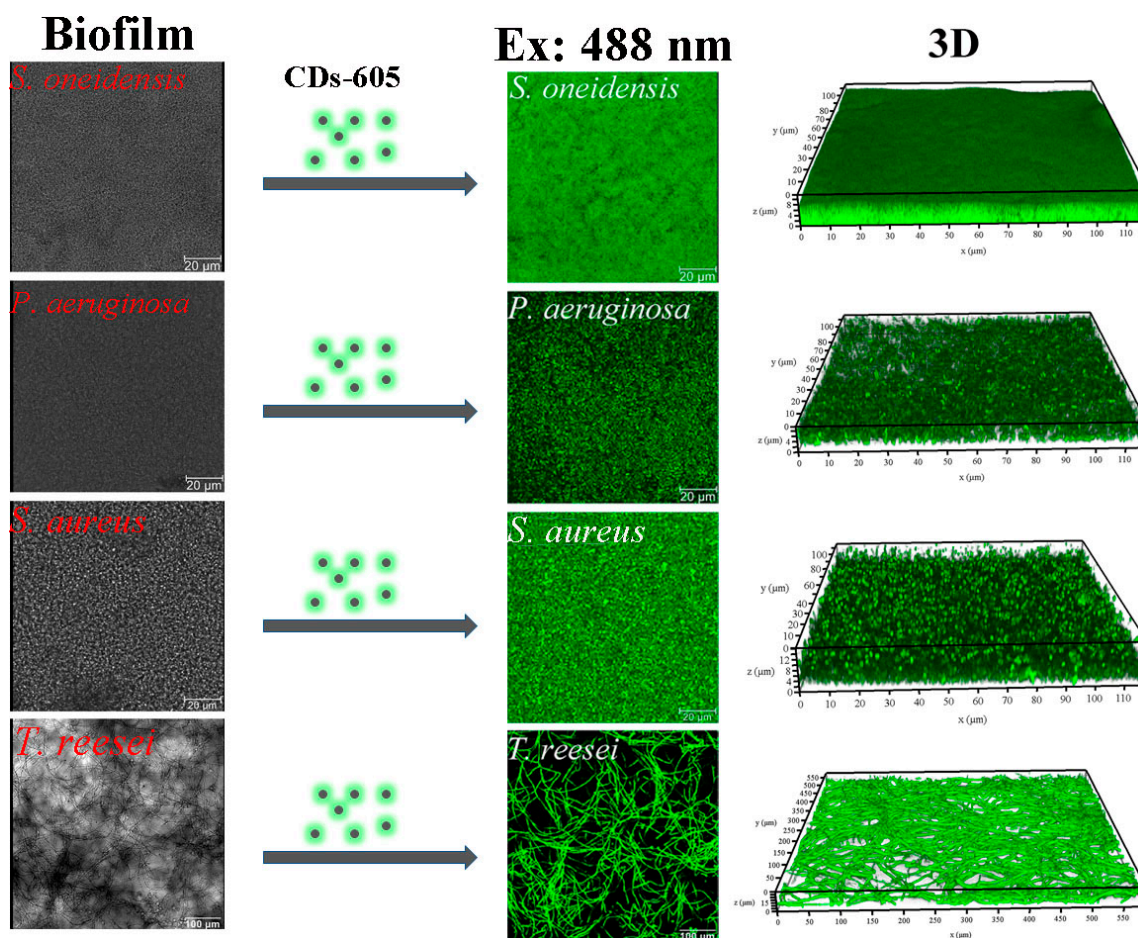


Figure 5. Confocal imaging results of biofilms formed by *S. oneidensis*, *P. aeruginosa*, *S. aureus*, and *T. reesei* using CDs-605. Reproduced with permission from [70]. Copyright Royal Society of Chemistry, 2017.

The above examples indicate that fluorescent CDs combined with fluorescence microscopy can realize in situ monitoring of both EPSs and embedded microorganisms in biofilms, representing a simple, yet powerful platform for biofilm imaging.

3. CDs for Killing Microorganisms

The antimicrobial activity of CDs has recently attracted much attention due to their excellent optical properties, low toxicity to mammalian cells, and multivalent interaction capability with microorganisms. The level of interaction between CDs and microorganisms depends on the composition, size, shape, and surface chemistry of the CDs, as well as the structure and surface chemistry of the microorganisms. In the following parts, we will discuss the killing of microorganisms using cationic CDs, uniquely shaped CDs, photosensitive CDs, antibiotic-modified CDs, and other CDs.

3.1. Positively Charged CDs

CDs with positive surface charge can interact with negatively charged bacteria, resulting in surface damage and cytoplasmic leakage of the bacteria and ultimately bacterial cell death. To obtain highly positively charged CDs, biogenic polyamines have been employed directly as precursors [71,72] or functionalization agents [73]. Polyamines such as spermine, spermidine, putrescine, and cadaverine are small molecules with two or more amine groups [74,75], which are ubiquitously produced in living cells with concentrations up to millimoles per liter. They are promising for application in surface modifications of nanomaterials due to their highly positive charge and great biocompatibility.

Positively charged spermine CDs (SC-dots) were synthesized from a mixture of glucose, spermine, and NaCl via microwave synthesis [71]. SC-dots displayed strong bactericidal activity. SC-dots possessed a zeta potential of +27.6 mV, allowing multivalent interaction with negatively charged bacteria and leading to cell surface damage. In addition, the interaction of SC-dots with bacteria increased the level of endogenous reactive oxygen species (ROS), contributing to their antimicrobial ability. Neutral CDs made from the same precursors without spermine showed no antimicrobial effect. Similarly, another type of super-cationic CDs (CQD_{Spds}) was obtained by direct pyrolysis of spermidine powder with dry heating treatment [72]. These ~6 nm, +45 mV CDs showed excellent bactericidal activity against both non-multidrug-resistant *E. coli*, *S. aureus*, *P. aeruginosa*, and *Salmonella enterica serovar Enteritidis* bacteria, and the multidrug-resistant bacterium, methicillin-resistant *S. aureus* (MRSA). The minimum inhibitory concentrations (MICs) of CQD_{Spds} for these tested microorganisms are ca. 2–4 µg/mL, ~2500-fold lower than that of free spermidine. Given that they displayed great biocompatibility both in vitro and in vivo, these CDs were successfully used for bacterial keratitis treatment, presenting a promising nanoantibiotic candidate for the topical treatment of eye-related bacterial infections. The CDs were found to damage the bacterial surfaces and bind to the bacterial DNA, thus causing the death of the bacteria. The positive charge of the CDs played a key role in their antibacterial action.

On the other hand, spermidine was used to functionalize CDs to endow them with highly positive charges [73]. Fluorescent carbon quantum dots (CQDs) were first prepared via pyrolysis of solid ammonium citrate and then linked with spermidine with heating treatment in the absence of coupling agents (Figure 6A). The obtained spermidine-capped CQDs (Spd-CQDs) with a zeta potential of +60.6 mV have excellent antimicrobial efficacy against both non-multidrug-resistant bacteria like *E. coli*, *S. aureus*, *B. subtilis*, and *P. aeruginosa*, and MRSA (Figure 6B). The MIC of Spd-CQDs is >25,000-fold and >10-fold lower than those of spermidine and CQD_{Spds} synthesized by direct pyrolysis of solid spermidine powder, respectively. With their high biocompatibility, Spd-CQDs were employed as a dressing material to heal MRSA-infected wounds in rats, leading to rapid healing, great epithelialization, and effective formation of collagen fibers (Figure 6C).

In addition to biogenic polyamines, antimicrobial cationic CDs were obtained from poly(ethyleneimine) [76], polyvinylpyrrolidone [77], 2,2'-(ethylenedioxy)bis(ethylamine) [28], and quaternary ammonium compounds [50,51]. Moreover, cationic CDs made from 2,2'-(ethylenedioxy)bis(ethylamine) [28], 3-ethoxypropylamine [28], curcumin [29], and benzoxazine monomers [30] displayed antiviral activities. Nevertheless, negatively charged CDs derived from 4-aminophenylboronic acid hydrochloride [26] and polyethylene glycol-diamine [27] have also been applied for antiviral applications successfully, suggesting that the positive charge of CDs is a beneficial but not necessary factor for their antiviral activities. Cationic CDs mainly interact with bacteria through electrostatic interaction, damage the cell walls/membranes, elicit cytoplasmic leakage, and ultimately kill the bacteria. Upon entering the cells, it is supposed that highly positively charged CDs damage the internal cytoplasmic membranes and interact with or cause lethal damage to nucleic acids. In addition, some cationic CDs can lead to the generation of ROS in the treated cells, but other CDs cannot [71]. All of these factors are responsible for the antimicrobial effect of cationic CDs.

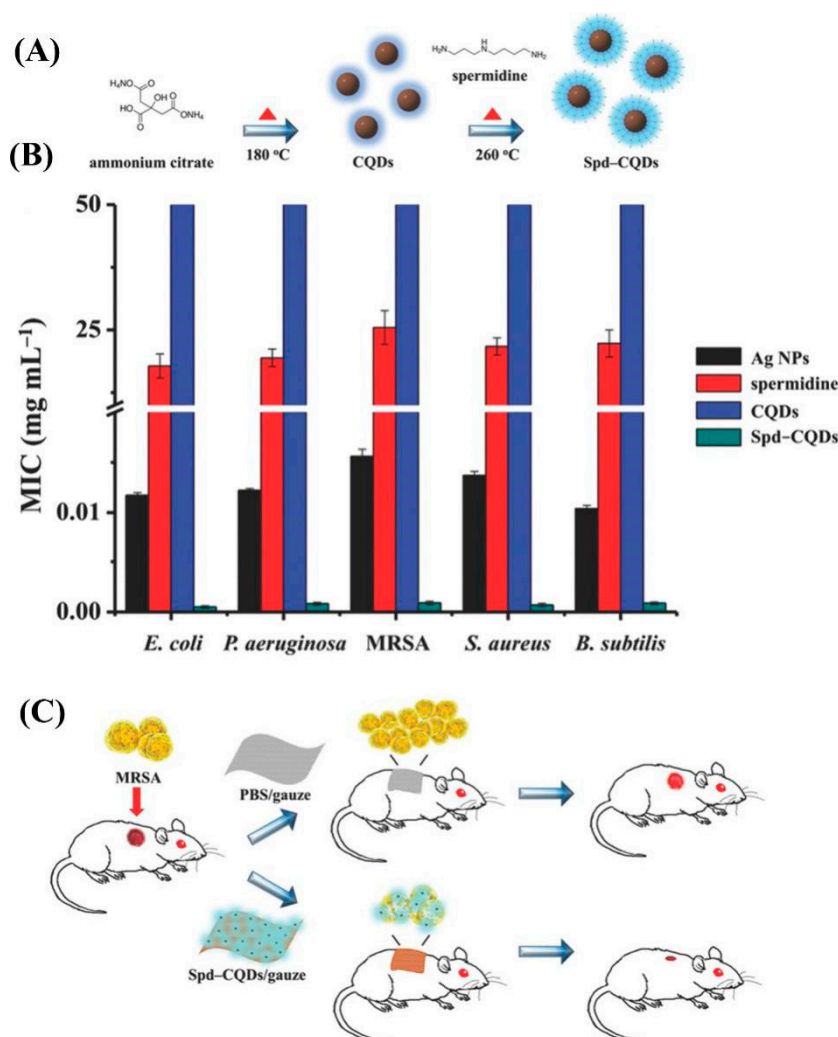


Figure 6. (A) Schematic illustration of the preparation of spermidine-functionalized carbon quantum dots (Spd-CQDs) from ammonium citrate and spermidine. (B) Minimum inhibitory concentrations (MICs) of silver nanoparticles (Ag NPs), spermidine, CQDs, and Spd-CQDs against five strains of bacteria. (C) Schematic presentation of the use of Spd-CQDs for wound healing. MRSA, methicillin-resistant *S. aureus*. Reproduced with permission from [73]. Copyright Wiley, 2016.

3.2. Uniquely Shaped CDs

It has been reported that the shape of CDs may affect their antimicrobial activity [78]. CDs synthesized by rupturing the C60 cage, namely C60-GQDs, showed exceptional antibacterial activity specifically against *S. aureus* [78]. C60-GQDs have a nonzero Gaussian curvature that matches well with that of the cell surface of *S. aureus*. The surface match ensures the association between C60-GQDs and *S. aureus*, resulting in damage to the cell envelope and the death of cells. In contrast, C60-GQD exhibited no bactericidal activity towards *B. subtilis*, *E. coli*, or *P. aeruginosa*. GQDs prepared from graphene oxide (GO-GQDs) with a planar geometry and zero Gaussian curvature possessed no antibacterial properties. The above results demonstrate that the surface of CDs may play a key role in their antimicrobial efficacy.

3.3. Photosensitive CDs

With their interaction with light, CDs display interesting responses, like charge/electron transfer, wavelength-dependent optical emissions, and heat generation, which can be applied for photocatalysis, bioimaging, and photomediated therapeutics. CDs have been successfully utilized as photoresponsive

agents for phototherapy (PT) to kill both cancer cells and microorganisms. The photodynamic therapy (PDT) and photothermal therapy (PTT) are the two main forms of PT.

3.3.1. PDT

PDT uses light to sensitize photosensitive agents (photosensitizers) in the presence of oxygen to produce ROS including singlet oxygen and free radicals, causing cell apoptosis/necrosis [79,80]. ROS can kill microorganisms by damaging DNA, oxidizing amino acids, and inactivating enzymes. PDT is considered to be a highly effective method for antibacterial and anticancer applications due to its fascinating merits, including antibiotic resistance independence, high spatial controllability, and low cumulative toxicity. Bare CDs and photosensitizer-conjugated CDs generate ROS upon light irradiation through the transfer of electrons or excitation energy to oxygen, serving as newly-minted photosensitizing nanoagents in PDT against cancers [81] and microorganisms [82–85].

Some CDs feature intrinsic photodynamic properties without any extra surface modifications, such as CDs prepared from graphene [82], poloxamer Pluronic F-68 [83], and mushroom [84]. QDs made from graphene via an electrochemical method produced ROS when photoexcited with blue light (470 nm, 1 W) and killed MRSA and *E. coli* [82]. Hydrophobic CQDs (hCQDs) were fabricated from a poloxamer Pluronic F-68 through bottom-up condensation [83]. hCQDs were utilized for the deposition of uniform and homogeneous Langmuir–Blodgett thin films (LB hCQDs thin films) on glass, SiO₂/Si, and mica substrates. Upon blue light (470 nm) irradiation, LB hCQDs thin films produced singlet oxygen and exhibited antibacterial and antibiofouling activity against four bacterial strains (*E. coli*, *S. aureus*, *Bacillus cereus*, and *P. aeruginosa*) (Figure 7A). These hCQDs were also embedded in a polyurethane polymer matrix, forming hCQDs/polyurethane nanocomposites by an easy swell–encapsulation–shrink approach [86]. Under blue light irradiation, hCQDs/polyurethane effectively generated singlet oxygen, which could diffuse from the polymer and kill the bacteria (Figure 7B). Such strategies are only suitable for treating skin and mucosal infections, as both blue light and visible light can be easily absorbed by tissues and have low tissue penetration.

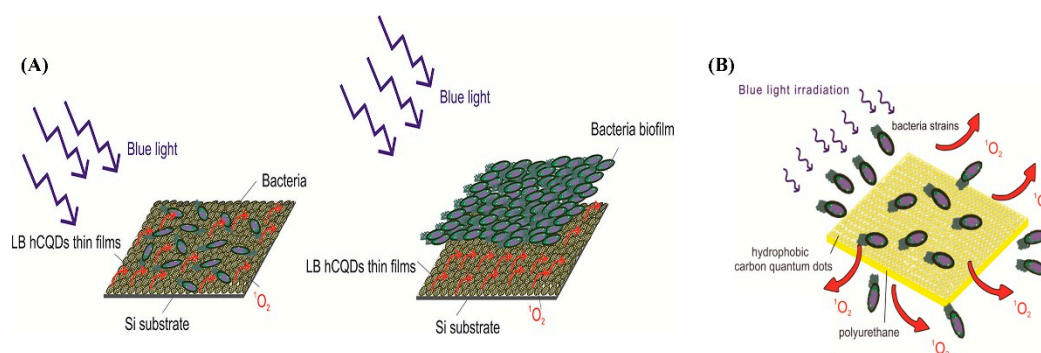


Figure 7. (A) Langmuir–Blodgett (LB) hCQDs thin films for both antibacterial and anti-biofilm photodynamic therapy (PDT). Reproduced with permission from [83]. Copyright American Chemical Society, 2018. (B) hCQDs/polyurethane for antibacterial PDT. Reproduced with permission from [86]. Copyright American Chemical Society, 2018.

Light at 700–1000 nm is more desirable for PDT and PTT because biological entities do not significantly absorb light in this range. To this end, CDs showing two-photon properties in the near-infrared (NIR) region have been developed. GO sheets were obtained through a modified Hummers' approach and were employed to synthesize QDs using an ultrasonic shearing reaction method [87]. In the NIR region, QDs exhibited high two-photon absorption, a wide cross section of two-photon excitation, strong two-photon luminescence, and excellent two-photon stability. Therefore, they could be used for both two-photon PDT and two-photon bioimaging toward both Gram-positive and Gram-negative bacteria, especially multidrug-resistant strains. The advantages of this method include ultralow laser energy, low delivered dose, and short photoexcitation time. The PDT performance of QDs can be improved by nitrogen

doping [88]. Nitrogen-doped GQDs (N-GQDs) with a higher nitrogen content could achieve better antimicrobial PDT performance. N-GQDs were further functionalized with amine groups, leading to amino-N-GQDs [89]. Amino-N-GQDs had superior capability for photodynamic antimicrobial therapy as compared to GQDs.

On the other hand, CDs can be modified with traditional PSs like methylene blue (MB) [90,91], protoporphyrin IX (PpIX) [92], and toluidine blue (TB) [91] for improved PDT against microorganisms. In addition, several CDs/metal oxide nanocomposites were fabricated and applied for antimicrobial PT, such as CDs/Cu₂O [93], CQDs–TiO₂ [94], ZnO/GQD [95], and CDs/Na₂W₄O₁₃/WO₃ [96]. Upon ultraviolet (UV)/visible light irradiation, all of these nanocomposites can produce ROS like singlet oxygen and/or free radicals to kill microorganisms. For example, Liu et al. synthesized ZnO/GQD nanocomposites via a hydrothermal method [95]. These nanocomposites displayed photo-improved antibacterial activity against *E. coli* under UV photo irradiation, as compared to ZnO and GQD. Using a similar synthetic strategy, Zhang et al. prepared carbon dots-decorated Na₂W₄O₁₃/WO₃ nanocomposites (CDs/Na₂W₄O₁₃/WO₃) [96], which exhibited remarkable antibacterial activity against *E. coli* upon visible light irradiation.

3.3.2. PTT

In addition to PDT, CDs can also be applied in antimicrobial PTT. In PTT, the administered photoresponsive agents absorb light to generate hyperthermia, causing cell damage and death. Sattarahmady et al. demonstrated that CDs made from hydrothermal treatment of ascorbic acid and copper acetate hydrate could convert NIR light to vibration energy to generate heat, causing temperature elevation in the suspensions containing CDs and bacteria [97]. The increased temperature led to ROS generation and cell wall damage, showing bactericidal effects toward *S. aureus* and MRSA. Although these CDs showed a negative zeta potential of -75 ± 4 mV, van der Waals forces could overcome the repulsion forces between these CDs and the negatively charged bacterial cell surface, resulting in their adhesion to the bacterial cell surface. The photothermal effect of CDs elicited toxicity against *S. aureus* and MRSA in a concentration-dependent way with cell wall disruption, high membrane permeability, high content diffusion, and oxidative stress. The bacterial growth was completely inhibited when the bacteria were treated with $7.0 \mu\text{g mL}^{-1}$ CDs and irradiated at a laser power density of 0.36 kJ cm^{-2} for 20 min. Despite being less explored than CD-based PDT, CD-based PTT represents a novel, promising strategy to fight against microorganisms as CDs exhibit advantageous properties like photostability, chemical stability, good water dispersibility, low toxicity, high biocompatibility, and eco-friendliness in comparison with some other semiconductor quantum dots [2].

3.4. Antibiotic-Modified CDs

The various functional groups on the surface of CDs enable the facile conjugation of the CDs with various antibiotics. To date, CDs have been modified with conventional antibiotics including ciprofloxacin [98,99], ampicillin [100], penicillin [101] vancomycin [92], and antiparasitic ointment [102] to kill microorganisms.

Fluorescent CDs prepared by microwave treatment of gum arabic were used as a carrier to deliver ciprofloxacin hydrochloride, a broad-spectrum antibiotic [98]. The antibiotic-conjugated CDs (Cipro@C-dots) could achieve controlled release of ciprofloxacin under physiological conditions, offering a solution to the problem of microbial resistance caused by overdosage of antibiotics. The conjugate displayed enhanced antimicrobial activity against both Gram-positive and Gram-negative bacteria. In another report, amine-functionalized CDs (CDs-NH₂) prepared by citric acid and ethylenediamine were covalently conjugated with ampicillin (AMP) through a cross-linking reaction between the primary amine groups of the CDs and the carboxyl groups of AMP, producing hybrid carbon nanomaterial CDs-AMP [100]. The immobilized AMP showed higher stability in solution and smaller MIC than the free one. CDs-AMP integrated the antibacterial effect of AMP with the intrinsic photodynamic property

of CDs, displaying effective inactivation of *E. coli* growth. Here, CDs are not only an antimicrobial agent but also a carrier for the delivery of AMP.

Moreover, CDs prepared using antibiotics directly as starting materials display antimicrobial activity. For example, water-dispersible, nontoxic, highly photoluminescent carbon nanodots (CNDs) were prepared by a green, simple hydrothermal approach from metronidazole, a kind of broad-spectrum antibiotic against obligate anaerobes [103]. CNDs possessed selective antibacterial activity against only obligate anaerobes as well as multicolor imaging capability. In another study, ciprofloxacin hydrochloride was used as a starting material to prepare self-functional graphitic carbon dots (g-CDs) via the hydrothermal method [99]. A reaction temperature of 200 °C was used to avoid the decomposition of ciprofloxacin to retain its functional structure on the surface of the as-synthesized g-CDs. The g-CDs exhibited high antibacterial activity against *S. aureus* and *E. coli*.

3.5. Metal-Based CDs as Antimicrobial Agents

CDs can be functionalized with metal-containing nanoparticles such as AgNPs [104,105], gold nanoparticles [24], and Ag–metal–organic framework (AgMOF) composites [106] to enhance their the antimicrobial activities. Habiba et al. prepared nanocomposites of GQD-decorated AgNPs using pulsed laser synthesis [104]. The obtained Ag-GQDs were further modified by poly(ethylene glycol) (PEG) to increase their biocompatibility and aqueous dispersity. The PEGylated Ag-GQDs exhibited higher antibacterial activity against both *S. aureus* and *P. aeruginosa* compared with bare GQDs and AgNPs alone. Priyadarshini et al. prepared CDs via microwave treatment of citric acid and PEG, which could reduce H₂AuCl₄ to obtain Au@CDs nanoconjugates [24]. Au@CDs inhibited the growth of the opportunistic fungal pathogen, *Candida albicans* (*C. albicans*). Recently, Travlou et al. fabricated AgMOF–CQD composites that exhibited high antibacterial activity against both Gram-positive and Gram-negative bacteria [106]. The authors pointed out that the formation of metallic silver and silver sulfides was essential for the antibacterial ability of AgMOF–CQDs.

3.6. Other CDs

CDs can exert selective antimicrobial effects through chiral molecular recognition [107] and peroxidase-like activity [108]. Xin et al. synthesized D-glutamic acid (D-Glu)-functionalized GQDs (DGGs) from citric acid and D-Glu via the hydrothermal method [107]. D-Glu is an essential molecule for biosynthesis of peptidoglycan (PG), an important component of bacterial cell wall but not mammalian cells. DGGs could damage the bacterial cell wall and enter the bacteria, showing high antibacterial efficacy against both Gram-negative and Gram-positive bacteria. DGGs were not toxic to mammalian cells, exhibiting exceptional biosafety. In contrast, L-glutamic acid (L-Glu)-functionalized GQDs (LGGs) displayed negligible toxicity to both bacteria and mammalian cells. In another report, Sun et al. fabricated GQDs from graphite via a modified Hummers' approach, which exhibited peroxidase-like activity that converted H₂O₂ into hydroxyl radical (•OH) for enhanced antibacterial activity against both Gram-negative (*E. coli*) and Gram-positive (*S. aureus*) bacteria [108].

On the other hand, developing degradable CDs is vital to decrease their biological toxicity. To this end, Li et al. fabricated degradable CDs from ascorbic acid using the one-step electrochemical method [25]. These CDs possessed broad-spectrum and high antimicrobial activity against both bacteria and fungi. The authors suggested that the CDs could diffuse into the microbial cells, damage their cell walls, bind to DNA and RNA, and influence the genetic process of these microorganisms. More importantly, these CDs could be completely degraded into CO₂, CO, and H₂O under visible light or at a mild temperature like 37 °C, ensuring their safe biomedical applications.

To summarize the Section 3, we have listed some representative CDs for killing various microorganisms in Table 1.

Table 1. Representative CDs for killing microorganisms.

| Precursor | Preparation | Microorganism | Ref. |
|---|---|--|-------|
| Cationic CDs | | | |
| Curcumin | Hydrothermal treatment | Porcine epidemic diarrhea virus | [29] |
| Glucose, spermine, and NaCl | Microwave synthesis | <i>E. coli</i> and <i>B. subtilis</i> | [71] |
| Spermidine | Dry heating treatment | Non-multidrug-resistant <i>E. coli</i> , <i>S. aureus</i> , <i>P. aeruginosa</i> , and <i>Salmonella enterica</i> serovar <i>Enteritidis</i> bacteria, and the multidrug-resistant bacterium, MRSA | [72] |
| Ammonium citrate and spermidine | Pyrolysis of solid ammonium citrate to make CDs that are linked with spermidine by heating treatment | Non-multidrug-resistant bacteria like <i>E. coli</i> , <i>S. aureus</i> , <i>B. subtilis</i> , and <i>P. aeruginosa</i> , and MRSA | [73] |
| Uniquely Shaped CDs | | | |
| C60 cage | Modified Hummers' method | <i>S. aureus</i> | [78] |
| Photosensitive CDs | | | |
| Graphene | Electrochemical method | MRSA and <i>E. coli</i> | [82] |
| Ploxamer Pluronic F-68 | Bottom-up condensation | <i>E. coli</i> , <i>S. aureus</i> , <i>Bacillus cereus</i> , and <i>P. aeruginosa</i> | [83] |
| Graphene oxide sheet | Ultrasonic shearing reaction method | <i>E. coli</i> and MRSA | [87] |
| Benzene and methylene blue | CDs were synthesized by focusing nanosecond laser pulses into benzene and were then combined with methylene blue | <i>E. coli</i> and <i>M. luteus</i> | [90] |
| Citric acid, zinc stearate, and diethylene glycol | Hydrothermal treatment | <i>E. coli</i> | [95] |
| Ascorbic acid and copper acetate hydrate | Hydrothermal treatment | <i>S. aureus</i> and MRSA | [97] |
| Antibiotic-Modified CDs | | | |
| Gum arabic and ciprofloxacin | CDs were prepared from gum arabic by microwave synthesis and conjugated with ciprofloxacin covalently | <i>B. subtilis</i> , <i>S. aureus</i> , <i>E. coli</i> and <i>P. aeruginosa</i> | [98] |
| Metronidazole | Hydrothermal treatment | <i>Porphyromonas gingivalis</i> | [103] |
| Metal-Based CDs | | | |
| Critic acid, PEG, and HAuCl ₄ | CDs were prepared via the microwave treatment of critic acid and PEG, which could reduce HAuCl ₄ to obtain Au@CDs nanoconjugates | <i>C. albicans</i> | [24] |
| Benzene, silver powder, and PEG | Pulsed laser synthesis | <i>S. aureus</i> and <i>P. aeruginosa</i> | [104] |
| Other CDs | | | |
| Ascorbic acid | Electrochemical method | <i>S. aureus</i> , <i>B. subtilis</i> , <i>Bacillus</i> sp. WL-6, <i>E. coli</i> , ampicillin-resistant <i>E. coli</i> , <i>R. solani</i> , and <i>P. grisea</i> | [25] |
| Citric acid and D-Glu | Hydrothermal treatment | <i>E. coli</i> and <i>S. aureus</i> | [107] |
| Graphite | Hummers' approach | <i>E. coli</i> and <i>S. aureus</i> | [108] |

4. Bacterial Theranostic Systems Based on CDs

Effective bacterial theranostic systems that integrate diagnostic functions and therapeutic effects have attracted extensive attention due to their excellent properties, including real-time monitoring capability, high efficiency, and ease of operation. Several kinds of fluorescent CDs have been developed for bacterial theranostics [50,87,109]. For example, Pramanik et al. integrated multicolor fluorescent CDs, magnetic nanoparticles, and the antimicrobial peptide pardaxin into one system and realized

efficient isolation, differentiation, and disinfection of superbugs in infected blood samples [109]. Specifically, fluorescent CDs (for imaging) were conjugated with magnetic nanoparticles (for isolation) by amide coupling. Then, antibodies as the specific binding unit for different superbugs were separately linked with fluorescent CDs to differentiate different superbugs. Finally, pardaxin was conjugated with magnetic nanoparticles for killing the superbugs. The multifunctional CDs successfully captured and killed MRSA and *Salmonella* DT104 superbugs in clinical samples.

5. Summary and Outlook

CDs are promising microbial imaging and antimicrobial agents due to their desired physicochemical and optical properties, including facile preparation, low toxicity, superior photostability, excellent water dispersibility, and flexible surface functionalization [110]. A large number of CDs have shown potent and consistent antimicrobial activity both in vitro and in vivo. For instance, some antibiotic-conjugated CDs can deliver and release the antibiotics to the specific sites of microbial cells to inactivate the cells. Some cationic CDs hold great potential to combat microbial infections and overcome drug resistance based on their strong capacity to interact with or disrupt the microbial cell walls/membranes. On the other hand, the facile synthesis and modification of CDs offer opportunities to precisely control their surface charges and functional groups, representing a huge advantage for developing new CDs with specific bactericidal activity against certain bacteria to solve the microbial multidrug-resistance issue. In addition, the controllable preparation and tunable optical properties of CDs will significantly benefit their future applications in biosystems. Nevertheless, there are still some challenges of CDs that may limit their practical applications. First, the photoluminescence mechanism of CDs remains unclear since their discovery in 2004, which severely limits the rational design of the CDs with desired fluorescence properties. Second, CDs with long excitation/emission wavelengths are still lacking, which impedes the applications of CDs in vivo and in thick biofilms due to the poor tissue/biofilm penetration capability of the CDs with short excitation/emission wavelengths. Third, many available CDs display multicolor emissions, possibly causing spectral overlap issues when two or more dyes are necessary for microbial imaging. Thus, fabricating CDs with single-color emission is also valuable for their practical applications. Fourth, the development of multifunctional CDs with desired size, composition, structure, and surface chemistry is urgently needed for more CD-based microbial theranostic applications. Especially, CDs that can selectively interact with a specific microbial strain have been seldom reported, which represents an important research direction for fabricating theranostic CDs. In this regard, new targeting ligands should be developed to modify the CDs, or CDs that have intrinsic microbial targeting capability need to be fabricated. Finally, for practical applications, large-scale synthesis and good biocompatibility of CDs are also vital for their cost-effective and safe application in microbial theranostics. Collectively, how to overcome the above-mentioned challenges becomes a future direction that is definitely worth exploring to improve the efficiency of CDs for sensing and killing microorganisms. With the future advancements in solving these challenges, we believe that CDs with better performance will find increasing applications in microbial theranostics.

Author Contributions: F.L. and F.-G.W. conceived and designed the review. F.L., Y.-W.B., and F.-G.W. drafted the manuscript.

Funding: This work was supported by the National Natural Science Foundation of China (31700040 and 21673037).

Acknowledgments: The authors appreciate the support of Southeast University and National Natural Science Foundation of China.

Conflicts of Interest: The authors declare no conflict of interest.

References

1. D'Costa, V.M.; King, C.E.; Kalan, L.; Morar, M.; Sung, W.W.L.; Schwarz, C.; Froese, D.; Zazula, G.; Calmels, F.; Debruyne, R.; et al. Antibiotic resistance is ancient. *Nature* **2011**, *477*, 457–461. [[CrossRef](#)] [[PubMed](#)]

2. Gao, G.; Jiang, Y.-W.; Sun, W.; Wu, F.-G. Fluorescent quantum dots for microbial imaging. *Chin. Chem. Lett.* **2018**, *29*, 1475–1485. [[CrossRef](#)]
3. Sun, W.; Wu, F.-G. Two-dimensional materials for antimicrobial applications: Graphene materials and beyond. *Chem.-Asian J.* **2018**, *13*, 3378–3410. [[CrossRef](#)] [[PubMed](#)]
4. Feng, H.; Qian, Z. Functional carbon quantum dots: A versatile platform for chemosensing and biosensing. *Chem. Rec.* **2018**, *18*, 491–505. [[CrossRef](#)] [[PubMed](#)]
5. Xu, X.; Ray, R.; Gu, Y.; Ploehn, H.J.; Gearheart, L.; Raker, K.; Scrivens, W.A. Electrophoretic analysis and purification of fluorescent single-walled carbon nanotube fragments. *J. Am. Chem. Soc.* **2004**, *126*, 12736–12737. [[CrossRef](#)] [[PubMed](#)]
6. Lin, F.; Li, C.; Chen, Z. Bacteria-derived carbon dots inhibit biofilm formation of *Escherichia coli* without affecting cell growth. *Front. Microbiol.* **2018**, *9*, 259. [[CrossRef](#)] [[PubMed](#)]
7. Yang, J.; Gao, G.; Zhang, X.; Ma, Y.-H.; Jia, H.-R.; Jiang, Y.-W.; Wang, Z.; Wu, F.-G. Ultrasmall and photostable nanotheranostic agents based on carbon quantum dots passivated with polyamine-containing organosilane molecules. *Nanoscale* **2017**, *9*, 15441–15452. [[CrossRef](#)] [[PubMed](#)]
8. Bao, Y.-W.; Hua, X.-W.; Li, Y.-H.; Jia, H.-R.; Wu, F.-G. Hyperthermia-promoted cytosolic and nuclear delivery of copper/carbon quantum dot-crosslinked nanosheets: Multimodal imaging-guided photothermal cancer therapy. *ACS Appl. Mater. Interfaces* **2018**, *10*, 1544–1555. [[CrossRef](#)]
9. Hua, X.-W.; Bao, Y.-W.; Zeng, J.; Wu, F.-G. Ultrasmall all-in-one nanodots formed via carbon dot-mediated and albumin-based synthesis: Multimodal imaging-guided and mild laser-enhanced cancer therapy. *ACS Appl. Mater. Interfaces* **2018**, *10*, 42077–42087. [[CrossRef](#)]
10. Hua, X.-W.; Bao, Y.-W.; Chen, Z.; Wu, F.-G. Carbon quantum dots with intrinsic mitochondrial targeting ability for mitochondria-based theranostics. *Nanoscale* **2017**, *9*, 10948–10960. [[CrossRef](#)]
11. Hua, X.-W.; Bao, Y.-W.; Wu, F.-G. Fluorescent carbon quantum dots with intrinsic nucleolus-targeting capability for nucleolus imaging and enhanced cytosolic and nuclear drug delivery. *ACS Appl. Mater. Interfaces* **2018**, *10*, 10664–10677. [[CrossRef](#)] [[PubMed](#)]
12. Teng, X.; Ma, C.; Ge, C.; Yan, M.; Yang, J.; Zhang, Y.; Morais, P.C.; Bi, H. Green synthesis of nitrogen-doped carbon dots from konjac flour with “off-on” fluorescence by Fe³⁺ and L-lysine for bioimaging. *J. Mater. Chem. B* **2014**, *2*, 4631–4639. [[CrossRef](#)]
13. Zhang, Y.; Shen, Y.; Teng, X.; Yan, M.; Bi, H.; Morais, P.C. Mitochondria-targeting nanoplateform with fluorescent carbon dots for long time imaging and magnetic field-enhanced cellular uptake. *ACS Appl. Mater. Interfaces* **2015**, *7*, 10201–10212. [[CrossRef](#)] [[PubMed](#)]
14. Gao, G.; Jiang, Y.-W.; Yang, J.; Wu, F.-G. Mitochondria-targetable carbon quantum dots for differentiating cancerous cells from normal cells. *Nanoscale* **2017**, *9*, 18368–18378. [[CrossRef](#)] [[PubMed](#)]
15. Gao, G.; Jiang, Y.-W.; Jia, H.-R.; Yang, J.; Wu, F.-G. On-off-on fluorescent nanosensor for Fe³⁺ detection and cancer/normal cell differentiation via silicon-doped carbon quantum dots. *Carbon* **2018**, *134*, 232–243. [[CrossRef](#)]
16. Hutton, G.A.M.; Martindale, B.C.M.; Reisner, E. Carbon dots as photosensitisers for solar-driven catalysis. *Chem. Soc. Rev.* **2017**, *46*, 6111–6123. [[CrossRef](#)] [[PubMed](#)]
17. Zhang, X.; Wang, J.; Liu, J.; Wu, J.; Chen, H.; Bi, H. Design and preparation of a ternary composite of graphene oxide/carbon dots/polypyrrole for supercapacitor application: Importance and unique role of carbon dots. *Carbon* **2017**, *115*, 134–146. [[CrossRef](#)]
18. Jaleel, J.A.; Pramod, K. Artful and multifaceted applications of carbon dot in biomedicine. *J. Control. Release* **2018**, *269*, 302–321. [[CrossRef](#)]
19. Lim, S.Y.; Shen, W.; Gao, Z. Carbon quantum dots and their applications. *Chem. Soc. Rev.* **2015**, *44*, 362–381. [[CrossRef](#)]
20. Kasibabu, B.S.B.; D’souza, S.L.; Jha, S.; Singhal, R.K.; Basu, H.; Kailasa, S.K. One-step synthesis of fluorescent carbon dots for imaging bacterial and fungal cells. *Anal. Methods* **2015**, *7*, 2373–2378. [[CrossRef](#)]
21. Mehta, V.N.; Jha, S.; Kailasa, S.K. One-pot green synthesis of carbon dots by using *Saccharum officinarum* juice for fluorescent imaging of bacteria (*Escherichia coli*) and yeast (*Saccharomyces cerevisiae*) cells. *Mater. Sci. Eng. C* **2014**, *38*, 20–27. [[CrossRef](#)] [[PubMed](#)]
22. Kasibabu, B.S.B.; D’souza, S.L.; Jha, S.; Kailasa, S.K. Imaging of bacterial and fungal cells using fluorescent carbon dots prepared from *Carica papaya* juice. *J. Fluoresc.* **2015**, *25*, 803–810. [[CrossRef](#)] [[PubMed](#)]

23. Hua, X.-W.; Bao, Y.-W.; Wang, H.-Y.; Chen, Z.; Wu, F.-G. Bacteria-derived fluorescent carbon dots for microbial live/dead differentiation. *Nanoscale* **2017**, *9*, 2150–2161. [[CrossRef](#)] [[PubMed](#)]
24. Priyadarshini, E.; Rawat, K.; Prasad, T.; Bohidar, H.B. Antifungal efficacy of Au@carbon dots nanoconjugates against opportunistic fungal pathogen, *Candida albicans*. *Colloid Surf. B-Biointerfaces* **2018**, *163*, 355–361. [[CrossRef](#)] [[PubMed](#)]
25. Li, H.; Huang, J.; Song, Y.; Zhang, M.; Wang, H.; Lu, F.; Huang, H.; Liu, Y.; Dai, X.; Gu, Z.; et al. Degradable carbon dots with broad-spectrum antibacterial activity. *ACS Appl. Mater. Interfaces* **2018**, *10*, 26936–26946. [[CrossRef](#)] [[PubMed](#)]
26. Barras, A.; Pagneux, Q.; Sane, F.; Wang, Q.; Boukherroub, R.; Hober, D.; Szunerits, S. High efficiency of functional carbon nanodots as entry inhibitors of herpes simplex virus type 1. *ACS Appl. Mater. Interfaces* **2016**, *8*, 9004–9013. [[CrossRef](#)]
27. Du, T.; Liang, J.; Dong, N.; Liu, L.; Fang, L.; Xiao, S.; Han, H. Carbon dots as inhibitors of virus by activation of type I interferon response. *Carbon* **2016**, *110*, 278–285. [[CrossRef](#)]
28. Dong, X.; Moyer, M.M.; Yang, F.; Sun, Y.P.; Yang, L. Carbon dots' antiviral functions against noroviruses. *Sci. Rep.* **2017**, *7*, 519. [[CrossRef](#)]
29. Ting, D.; Dong, N.; Fang, L.; Lu, J.; Bi, J.; Xiao, S.; Han, H. Multisite inhibitors for enteric coronavirus: Antiviral cationic carbon dots based on curcumin. *ACS Appl. Nano Mater.* **2018**, *1*, 5451–5459. [[CrossRef](#)]
30. Huang, S.; Gu, J.; Ye, J.; Fang, B.; Wan, S.; Wang, C.; Ashraf, U.; Li, Q.; Shao, L.; Song, Y.; et al. Benzoxazine monomer derived carbon dots as a broad-spectrum agent to block viral infectivity. *J. Colloid Interface Sci.* **2019**, *542*, 198–206. [[CrossRef](#)]
31. Sharma, V.; Tiwari, P.; Mobin, S.M. Sustainable carbon-dots: Recent advances in green carbon dots for sensing and bioimaging. *J. Mater. Chem. B* **2017**, *5*, 8904–8924. [[CrossRef](#)]
32. Chandra, S.; Mahto, T.K.; Chowdhuri, A.R.; Das, B.; Sahu, S.K. One step synthesis of functionalized carbon dots for the ultrasensitive detection of *Escherichia coli* and iron(III). *Sens. Actuators B* **2017**, *245*, 835–844. [[CrossRef](#)]
33. Chandra, S.; Chowdhuri, A.R.; Mahto, T.K.; Samui, A.; Sahu, S.K. One-step synthesis of amikacin modified fluorescent carbon dots for the detection of Gram-negative bacteria like *Escherichia coli*. *RSC Adv.* **2016**, *6*, 72471–72478. [[CrossRef](#)]
34. Bhattacharya, S.; Nandi, S.; Jelinek, R. Carbon-dot–hydrogel for enzyme-mediated bacterial detection. *RSC Adv.* **2017**, *7*, 588–594. [[CrossRef](#)]
35. Bhaire, M.L.; Gedda, G.; Khan, M.S.; Wu, H.-F. Fluorimetric detection of pathogenic bacteria using magnetic carbon dots. *Anal. Chim. Acta* **2016**, *920*, 63–71. [[CrossRef](#)]
36. Baig, M.M.F.; Chen, Y.-C. Bright carbon dots as fluorescence sensing agents for bacteria and curcumin. *J. Colloid Interface Sci.* **2017**, *501*, 341–349. [[CrossRef](#)]
37. Mandal, T.K.; Parvin, N. Rapid detection of bacteria by carbon quantum dots. *J. Biomed. Nanotechnol.* **2011**, *7*, 846–848. [[CrossRef](#)]
38. Tripathi, K.M.; Sonker, A.K.; Sonkar, S.K.; Sarkar, S. Pollutant soot of diesel engine exhaust transformed to carbon dots for multicoloured imaging of *E. coli* and sensing cholesterol. *RSC Adv.* **2014**, *4*, 30100–30107. [[CrossRef](#)]
39. Wang, N.; Fan, H.; Sun, J.; Han, Z.; Dong, J.; Ai, S. Fluorine-doped carbon nitride quantum dots: Ethylene glycol-assisted synthesis, fluorescent properties, and their application for bacterial imaging. *Carbon* **2016**, *109*, 141–148. [[CrossRef](#)]
40. Zhang, Y.; Liu, X.; Fan, Y.; Guo, X.; Zhou, L.; Lv, Y.; Lin, J. One-step microwave synthesis of N-doped hydroxyl-functionalized carbon dots with ultra-high fluorescence quantum yields. *Nanoscale* **2016**, *8*, 15281–15287. [[CrossRef](#)]
41. Nandi, S.; Ritenberg, M.; Jelinek, R. Bacterial detection with amphiphilic carbon dots. *Analyst* **2015**, *140*, 4232–4237. [[CrossRef](#)] [[PubMed](#)]
42. Cao, L.; Wang, X.; Mezziani, M.J.; Lu, F.; Wang, H.; Luo, P.G.; Lin, Y.; Harruff, B.A.; Veca, L.M.; Murray, D.; et al. Carbon dots for multiphoton bioimaging. *J. Am. Chem. Soc.* **2007**, *129*, 11318–11319. [[CrossRef](#)] [[PubMed](#)]
43. Nandi, S.; Malishev, R.; Kootery, K.P.; Mirsky, Y.; Kolusheva, S.; Jelinek, R. Membrane analysis with amphiphilic carbon dots. *Chem. Commun.* **2014**, *50*, 10299–10302. [[CrossRef](#)] [[PubMed](#)]
44. Cayuela, A.; Kennedy, S.R.; Soriano, M.L.; Jones, C.D.; Valcárcel, M.; Steed, J.W. Fluorescent carbon dot–molecular salt hydrogels. *Chem. Sci.* **2015**, *6*, 6139–6146. [[CrossRef](#)] [[PubMed](#)]

45. Gogoi, N.; Barooah, M.; Majumdar, G.; Chowdhury, D. Carbon dots rooted agarose hydrogel hybrid platform for optical detection and separation of heavy metal ions. *ACS Appl. Nano Mater* **2015**, *7*, 3058–3067. [[CrossRef](#)] [[PubMed](#)]
46. Ding, C.; Zhu, A.; Tian, Y. Functional surface engineering of C-dots for fluorescent biosensing and in vivo bioimaging. *Acc. Chem. Res.* **2014**, *47*, 20–30. [[CrossRef](#)] [[PubMed](#)]
47. Weng, C.-I.; Chang, H.-T.; Lin, C.-H.; Shen, Y.-W.; Unnikrishnan, B.; Li, Y.-J.; Huang, C.-C. One-step synthesis of biofunctional carbon quantum dots for bacterial labeling. *Biosens. Bioelectron.* **2015**, *68*, 1–6. [[CrossRef](#)]
48. Nugent, R.P.; Krohn, M.A.; Hillier, S.L. Reliability of diagnosing bacterial vaginosis is improved by a standardized method of gram stain interpretation. *J. Clin. Microbiol.* **1991**, *29*, 297–301.
49. Zhong, D.; Zhuo, Y.; Feng, Y.; Yang, X. Employing carbon dots modified with vancomycin for assaying Gram-positive bacteria like *Staphylococcus aureus*. *Biosens. Bioelectron.* **2015**, *74*, 546–553. [[CrossRef](#)]
50. Yang, J.; Zhang, X.; Ma, Y.-H.; Gao, G.; Chen, X.; Jia, H.-R.; Li, Y.-H.; Chen, Z.; Wu, F.-G. Carbon dot-based platform for simultaneous bacterial distinguishment and antibacterial applications. *ACS Appl. Mater. Interfaces* **2016**, *8*, 32170–32181. [[CrossRef](#)]
51. Yang, J.; Gao, G.; Zhang, X.; Ma, Y.-H.; Chen, X.; Wu, F.-G. One-step synthesized carbon dots with bacterial contact-enhanced fluorescence emission property: Fast Gram-type identification and selective Gram-positive bacterial inactivation. *Carbon* **2019**, *146*, 827–839. [[CrossRef](#)]
52. Zhao, E.; Hong, Y.; Chen, S.; Leung, C.W.T.; Chan, C.Y.K.; Kwok, R.T.K.; Lam, J.W.Y.; Tang, B.Z. Highly fluorescent and photostable probe for long-term bacterial viability assay based on aggregation-induced emission. *Adv. Healthc. Mater.* **2014**, *3*, 88–96. [[CrossRef](#)] [[PubMed](#)]
53. Keer, J.T.; Birch, L. Molecular methods for the assessment of bacterial viability. *J. Microbiol. Methods* **2003**, *53*, 175–183. [[CrossRef](#)]
54. Gu, Y.; Hu, Y.; Zhao, X.; Chen, X.; Wang, P.; Zheng, Z. Discrimination of viable and dead microbial materials with Fourier transform infrared spectroscopy in 3–5 micrometers. *Opt. Express* **2018**, *26*, 15842–15850. [[CrossRef](#)] [[PubMed](#)]
55. Fantner, G.E.; Barbero, R.J.; Gray, D.S.; Belcher, A.M. Kinetics of antimicrobial peptide activity measured on individual bacterial cells using high-speed atomic force microscopy. *Nat. Nanotechnol.* **2010**, *5*, 280–285. [[CrossRef](#)]
56. Zhou, H.; Yang, D.; Ivleva, N.P.; Mircescu, N.E.; Schubert, S.; Niessner, R.; Wieser, A.; Haisch, C. Label-free in situ discrimination of live and dead bacteria by surface-enhanced Raman scattering. *Anal. Chem.* **2015**, *87*, 6553–6561. [[CrossRef](#)]
57. Song, Y.; Li, H.; Lu, F.; Wang, H.; Zhang, M.; Yang, J.; Huang, J.; Huang, H.; Liu, Y.; Kang, Z. Fluorescent carbon dots with highly negative charges as a sensitive probe for real-time monitoring of bacterial viability. *J. Mater. Chem. B* **2017**, *5*, 6008–6015. [[CrossRef](#)]
58. Lu, F.; Song, Y.; Huang, H.; Liu, Y.; Fu, Y.; Huang, J.; Li, H.; Qu, H.; Kang, Z. Fluorescent carbon dots with tunable negative charges for bio-imaging in bacterial viability assessment. *Carbon* **2017**, *120*, 95–102. [[CrossRef](#)]
59. Lin, F.; Li, C.; Chen, Z. Exopolysaccharide-derived carbon dots for microbial viability assessment. *Front. Microbiol.* **2018**, *9*, 2697. [[CrossRef](#)]
60. Flemming, H.-C.; Wingender, J. The biofilm matrix. *Nat. Rev. Microbiol.* **2010**, *8*, 623–633. [[CrossRef](#)]
61. Mah, T.F.; Pitts, B.; Pellock, B.; Walker, G.C.; Stewart, P.S.; O’Toole, G.A. A genetic basis for *Pseudomonas aeruginosa* biofilm antibiotic resistance. *Nature* **2003**, *426*, 306–310. [[CrossRef](#)] [[PubMed](#)]
62. Duncan, B.; Li, X.; Landis, R.F.; Kim, S.T.; Gupta, A.; Wang, L.-S.; Ramanathan, R.; Tang, R.; Boerth, J.A.; Rotello, V.M. Nanoparticle-stabilized capsules for the treatment of bacterial biofilms. *ACS Nano* **2015**, *9*, 7775–7782. [[CrossRef](#)]
63. Natalio, F.; André, R.; Hartog, A.F.; Stoll, B.; Jochum, K.P.; Wever, R.; Tremel, W. Vanadium pentoxide nanoparticles mimic vanadium haloperoxidases and thwart biofilm formation. *Nat. Nanotechnol.* **2012**, *7*, 530–535. [[CrossRef](#)] [[PubMed](#)]
64. Denkhaus, E.; Meisen, S.; Telgheder, U.; Wingender, J. Chemical and physical methods for characterisation of biofilms. *Microchim. Acta* **2007**, *158*, 1–27. [[CrossRef](#)]
65. Wolf, G.; Crespo, J.G.; Reis, M.A.M. Optical and spectroscopic methods for biofilm examination and monitoring. *Rev. Environ. Sci. Biotechnol.* **2002**, *1*, 227–251. [[CrossRef](#)]

66. Neu, T.R.; Swerhone, G.D.W.; Lawrence, J.R. Assessment of lectin-binding analysis for in situ detection of glycoconjugates in biofilm systems. *Microbiology* **2001**, *147*, 299–313. [[CrossRef](#)] [[PubMed](#)]
67. Aldeek, F.; Mustin, C.; Balan, L.; Roques-Carmes, T.; Fontaine-Aupart, M.-P.; Schneider, R. Surface-engineered quantum dots for the labeling of hydrophobic microdomains in bacterial biofilms. *Biomaterials* **2011**, *32*, 5459–5470. [[CrossRef](#)]
68. Chalmers, N.I.; Palmer, R.J.; Du-Thumm, L.; Sullivan, R.; Shi, W.; Kolenbrander, P.E. Use of quantum dot luminescent probes to achieve single-cell resolution of human oral bacteria in biofilms. *Appl. Environ. Microbiol.* **2007**, *73*, 630–636. [[CrossRef](#)]
69. Ritenberg, M.; Nandi, S.; Kolusheva, S.; Dandela, R.; Meijler, M.M.; Jelinek, R. Imaging *Pseudomonas aeruginosa* biofilm extracellular polymer scaffolds with amphiphilic carbon dots. *ACS Chem. Biol.* **2016**, *11*, 1265–1270. [[CrossRef](#)]
70. Lin, F.; Li, C.; Dong, L.; Fu, D.; Chen, Z. Imaging biofilm-encased microorganisms using carbon dots derived from *L. plantarum*. *Nanoscale* **2017**, *9*, 9056–9064. [[CrossRef](#)]
71. Bing, W.; Sun, H.J.; Yan, Z.; Ren, J.; Qu, X. Programmed bacteria death induced by carbon dots with different surface charge. *Small* **2016**, *12*, 4713–4718. [[CrossRef](#)] [[PubMed](#)]
72. Jian, H.-J.; Wu, R.-S.; Lin, T.-Y.; Li, Y.-J.; Lin, H.-J.; Harroun, S.G.; Lai, J.-Y.; Huang, C.-C. Super-cationic carbon quantum dots synthesized from spermidine as an eye drop formulation for topical treatment of bacterial keratitis. *ACS Nano* **2017**, *11*, 6703–6716. [[CrossRef](#)] [[PubMed](#)]
73. Li, Y.-J.; Harroun, S.G.; Su, Y.-C.; Huang, C.-F.; Unnikrishnan, B.; Lin, H.-J.; Lin, C.-H.; Huang, C.-C. Synthesis of self-assembled spermidine-carbon quantum dots effective against multidrug-resistant bacteria. *Adv. Healthc. Mater.* **2016**, *5*, 2545–2554. [[CrossRef](#)] [[PubMed](#)]
74. Michael, A.J. Polyamines in eukaryotes, bacteria, and archaea. *J. Biol. Chem.* **2016**, *291*, 14896–14903. [[CrossRef](#)] [[PubMed](#)]
75. Pegg, A.E. Functions of polyamines in mammals. *J. Biol. Chem.* **2016**, *291*, 14904–14912. [[CrossRef](#)] [[PubMed](#)]
76. Dou, Q.; Fang, X.; Jiang, S.; Chee, P.L.; Lee, T.-C.; Loh, X.J. Multi-functional fluorescent carbon dots with antibacterial and gene delivery properties. *RSC Adv.* **2015**, *5*, 46817–46822. [[CrossRef](#)]
77. Travlou, N.A.; Giannakoudakis, D.A.; Algarra, M.; Labella, A.M.; Rodríguez-Castellón, E.; Bandosz, T.J. S- and N-doped carbon quantum dots: Surface chemistry dependent antibacterial activity. *Carbon* **2018**, *135*, 104–111. [[CrossRef](#)]
78. Hui, L.; Huang, J.; Chen, G.; Zhu, Y.; Yang, L. Antibacterial property of graphene quantum dots (both source material and bacterial shape matter). *ACS Appl. Mater. Interfaces* **2016**, *8*, 20–25. [[CrossRef](#)]
79. Li, C.; Lin, F.; Sun, W.; Wu, F.-G.; Yang, H.; Lv, R.; Zhu, Y.-X.; Jia, H.-R.; Wang, C.; Gao, G.; et al. Self-assembled rose bengal-exopolysaccharide nanoparticles for improved photodynamic inactivation of bacteria by enhancing singlet oxygen generation directly in the solution. *ACS Appl. Mater. Interfaces* **2018**, *10*, 16715–16722. [[CrossRef](#)]
80. Lin, F.; Bao, Y.-W.; Wu, F.-G. Improving the phototherapeutic efficiencies of molecular and nanoscale materials by targeting mitochondria. *Molecules* **2018**, *23*, 3016. [[CrossRef](#)]
81. Ge, J.; Lan, M.; Zhou, B.; Liu, W.; Guo, L.; Wang, H.; Jia, Q.; Niu, G.; Huang, X.; Zhou, H.; et al. A graphene quantum dot photodynamic therapy agent with high singlet oxygen generation. *Nat. Commun.* **2014**, *5*, 4596. [[CrossRef](#)] [[PubMed](#)]
82. Ristic, B.Z.; Milenkovic, M.M.; Dakic, I.R.; Todorovic-Markovic, B.M.; Milosavljevic, M.S.; Budimir, M.D.; Paunovic, V.G.; Dramicanin, M.D.; Markovic, Z.M.; Trajkovic, V.S. Photodynamic antibacterial effect of graphene quantum dots. *Biomaterials* **2014**, *35*, 4428–4435. [[CrossRef](#)] [[PubMed](#)]
83. Stanković, N.K.; Bodik, M.; Šiffalovič, P.; Kotlar, M.; Mičušik, M.; Špitalsky, Z.; Danko, M.; Milivojević, D.D.; Kleinova, A.; Kubat, P.; et al. Antibacterial and antibiofouling properties of light triggered fluorescent hydrophobic carbon quantum dots Langmuir–Blodgett thin films. *ACS Sustain. Chem. Eng.* **2018**, *6*, 4154–4163. [[CrossRef](#)]
84. Venkateswarlu, S.; Viswanath, B.; Reddy, A.S.; Yoon, M. Fungus-derived photoluminescent carbon nanodots for ultrasensitive detection of Hg²⁺ ions and photoinduced bactericidal activity. *Sens. Actuator B-Chem.* **2018**, *258*, 172–183. [[CrossRef](#)]
85. Dong, X.; Awak, M.A.; Wang, P.; Sun, Y.-P.; Yang, L. Carbon dot incorporated multi-walled carbon nanotube coated filters for bacterial removal and inactivation. *RSC Adv.* **2018**, *8*, 8292–8301. [[CrossRef](#)] [[PubMed](#)]

86. Kováčová, M.; Marković, Z.M.; Humpolíček, P.; Mičušík, M.; Švajdlenková, H.; Kleinová, A.; Danko, M.; Kubát, P.; Vajdák, J.; Capáková, Z.; et al. Carbon quantum dots modified polyurethane nanocomposite as effective photocatalytic and antibacterial agents. *ACS Biomater. Sci. Eng.* **2018**, *4*, 3983–3993. [[CrossRef](#)]
87. Kuo, W.-S.; Chang, C.-Y.; Chen, H.-H.; Hsu, C.-L.L.; Wang, J.-Y.; Kao, H.-F.; Chou, L.C.-S.; Chen, Y.-C.; Chen, S.-J.; Chang, W.-T.; et al. Two-photon photoexcited photodynamic therapy and contrast agent with antimicrobial graphene quantum dots. *ACS Appl. Mater. Interfaces* **2016**, *8*, 30467–30474. [[CrossRef](#)]
88. Kuo, W.-S.; Chen, H.-H.; Chen, S.-Y.; Chang, C.-Y.; Chen, P.-C.; Hou, Y.-I.; Shao, Y.-T.; Kao, H.-F.; Hsu, C.-L.L.; Chen, Y.-C.; et al. Graphene quantum dots with nitrogen-doped content dependence for highly efficient dual-modality photodynamic antimicrobial therapy and bioimaging. *Biomaterials* **2017**, *120*, 185–194. [[CrossRef](#)]
89. Kuo, W.-S.; Shao, Y.-T.; Huang, K.-S.; Chou, T.-M.; Yang, C.-H. Antimicrobial amino-functionalized nitrogen-doped graphene quantum dots for eliminating multidrug-resistant species in dual-modality photodynamic therapy and bioimaging under two-photon excitation. *ACS Appl. Mater. Interfaces* **2018**, *10*, 14438–14446. [[CrossRef](#)]
90. Kholikov, K.; Ilhom, S.; Sajjad, M.; Smith, M.E.; Monroe, J.D.; San, O.; Er, A.O. Improved singlet oxygen generation and antimicrobial activity of sulphur-doped graphene quantum dots coupled with methylene blue for photodynamic therapy applications. *Photodiagnosis Photodyn. Ther.* **2018**, *24*, 7–14. [[CrossRef](#)]
91. Dong, X.; Bond, A.E.; Pan, N.; Coleman, M.; Tang, Y.; Sun, Y.-P.; Yang, L. Synergistic photoactivated antimicrobial effects of carbon dots combined with dye photosensitizers. *Int. J. Nanomed.* **2018**, *13*, 8025–8035. [[CrossRef](#)] [[PubMed](#)]
92. Pan, C.-L.; Chen, M.-H.; Tung, F.-I.; Liu, T.-Y. A nanovehicle developed for treating deep-seated bacteria using low-dose X-ray. *Acta Biomater.* **2017**, *47*, 159–169. [[CrossRef](#)] [[PubMed](#)]
93. De, B.; Gupta, K.; Mandal, M.; Karak, N. Biocide immobilized OMMT-carbon dot reduced Cu₂O nanohybrid/hyperbranched epoxy nanocomposites: Mechanical, thermal, antimicrobial and optical properties. *Mater. Sci. Eng. C-Mater. Biol. Appl.* **2015**, *56*, 74–83. [[CrossRef](#)] [[PubMed](#)]
94. Yan, Y.; Kuang, W.; Shi, L.; Ye, X.; Yang, Y.; Xie, X.; Shi, Q.; Tan, S. Carbon quantum dot-decorated TiO₂ for fast and sustainable antibacterial properties under visible-light. *J. Alloys Compd.* **2019**, *777*, 234–243. [[CrossRef](#)]
95. Liu, J.; Rojas-Andrade, M.D.; Chata, G.; Peng, Y.; Roseman, G.; Lu, J.-E.; Millhauser, G.L.; Saltikov, C.; Chen, S. Photo-enhanced antibacterial activity of ZnO/graphene quantum dot nanocomposites. *Nanoscale* **2018**, *10*, 158–166. [[CrossRef](#)] [[PubMed](#)]
96. Zhang, J.; Liu, X.; Wang, X.; Mu, L.; Yuan, M.; Liu, B.; Shi, H. Carbon dots-decorated Na₂W₄O₁₃ composite with WO₃ for highly efficient photocatalytic antibacterial activity. *J. Hazard. Mater.* **2018**, *359*, 1–8. [[CrossRef](#)] [[PubMed](#)]
97. Sattarahmady, N.; Rezaie-Yazdi, M.; Tondro, G.H.; Akbari, N. Bactericidal laser ablation of carbon dots: An in vitro study on wild-type and antibiotic-resistant *Staphylococcus aureus*. *J. Photochem. Photobiol. B-Biol.* **2017**, *166*, 323–332. [[CrossRef](#)]
98. Thakur, M.; Pandey, S.; Mewada, A.; Patil, V.; Khade, M.; Goshi, E.; Sharon, M. Antibiotic conjugated fluorescent carbon dots as a theranostic agent for controlled drug release, bioimaging, and enhanced antimicrobial activity. *J. Drug Deliv.* **2014**, *2014*, 282193. [[CrossRef](#)]
99. Hou, P.; Yang, T.; Liu, H.; Li, Y.F.; Huang, C.Z. An active structure preservation method for developing functional graphitic carbon dots as an effective antibacterial agent and a sensitive pH and Al(III) nanosensor. *Nanoscale* **2017**, *9*, 17334–17341. [[CrossRef](#)]
100. Jijie, R.; Barras, A.; Bouckaert, J.; Dumitrascu, N.; Szunerits, S.; Boukherroub, R. Enhanced antibacterial activity of carbon dots functionalized with ampicillin combined with visible light triggered photodynamic effects. *Colloid Surf. B-Biointerfaces* **2018**, *170*, 347–354. [[CrossRef](#)]
101. Sidhu, J.S.; Mayank; Pandiyan, T.; Kaur, N.; Singh, N. The photochemical degradation of bacterial cell wall using penicillin-based carbon dots: Weapons against multi-drug resistant (MDR) strains. *ChemistrySelect* **2017**, *2*, 9277–9283. [[CrossRef](#)]
102. Kumar, V.B.; Dolitzky, A.; Michaeli, S.; Gedanken, A. Antiparasitic ointment based on a biocompatible carbon dot nanocomposite. *ACS Appl. Nano Mater.* **2018**, *1*, 1784–1791. [[CrossRef](#)]
103. Liu, J.; Lu, S.; Tang, Q.; Zhang, K.; Yu, W.; Sun, H.; Yang, B. One-step hydrothermal synthesis of photoluminescent carbon nanodots with selective antibacterial activity against *Porphyromonas gingivalis*. *Nanoscale* **2017**, *9*, 7135–7142. [[CrossRef](#)] [[PubMed](#)]

104. Habiba, K.; Bracho-Rincon, D.P.; Gonzalez-Feliciano, J.A.; Villalobos-Santos, J.C.; Makarov, V.I.; Ortiz, D.; Avalos, J.A.; Gonzalez, C.I.; Weiner, B.R.; Morell, G. Synergistic antibacterial activity of PEGylated silver–graphene quantum dots nanocomposites. *Appl. Mater. Today* **2015**, *1*, 80–87. [[CrossRef](#)]
105. Han, S.; Zhang, H.; Xie, Y.; Liu, L.; Shan, C.; Li, X.; Liu, W.; Tang, Y. Application of cow milk-derived carbon dots/AgNPs composite as the antibacterial agent. *Appl. Surf. Sci.* **2015**, *328*, 368–373. [[CrossRef](#)]
106. Travlou, N.A.; Algarra, M.; Alcoholado, C.; Cifuentes-Rueda, M.; Labella, A.M.; Lázaro-Martínez, J.M.; Rodríguez-Castellón, E.; Bandosz, T.J. Carbon quantum dot surface-chemistry-dependent Ag release governs the high antibacterial activity of Ag-metal–organic framework composites. *ACS Appl. Bio Mater.* **2018**, *1*, 693–707. [[CrossRef](#)]
107. Xin, Q.; Liu, Q.; Geng, L.; Fang, Q.; Gong, J.R. Chiral nanoparticle as a new efficient antimicrobial nanoagent. *Adv. Healthc. Mater.* **2017**, *6*, 1601011. [[CrossRef](#)] [[PubMed](#)]
108. Sun, H.; Gao, N.; Dong, K.; Ren, J.; Qu, X. Graphene quantum dots-band-aids used for wound disinfection. *ACS Nano* **2014**, *8*, 6202–6210. [[CrossRef](#)]
109. Pramanik, A.; Jones, S.; Pedraza, F.; Vangara, A.; Sweet, C.; Williams, M.S.; Ruppia-Kasani, V.; Risher, S.E.; Sardar, D.; Ray, P.C. Fluorescent, magnetic multifunctional carbon dots for selective separation, identification, and eradication of drug-resistant superbugs. *ACS Omega* **2017**, *2*, 554–562. [[CrossRef](#)]
110. Wang, Y.; Hu, A. Carbon quantum dots: Synthesis, properties and applications. *J. Mater. Chem. C* **2014**, *2*, 6921–6939. [[CrossRef](#)]



© 2019 by the authors. Licensee MDPI, Basel, Switzerland. This article is an open access article distributed under the terms and conditions of the Creative Commons Attribution (CC BY) license (<http://creativecommons.org/licenses/by/4.0/>).